Eur. Phys. J. D (2024)78:94
https://doi.org/10.1140/epjd/s10053-024-00889-5

THE EUROPEAN PHYSICAL JOURNAL D

Regular Article - Optical Phenomena and Photonics

Saturation and absorption effects on the transmission properties of Kerr-type nonlinear layers

C. A. Betancur-Yepes[1,a], J. D. Mazo-Vásquez[2,b], and E. Reyes-Gómez[1,c]

[1] Instituto de Física, Universidad de Antioquia UdeA, Calle 70 No. 52-21, Medellín, Colombia
[2] Department of Physics, Karlsruhe Institute of Technology, Wolfgang-Gaede-Str. 1, D-76131 Karlsruhe, Germany

Received 22 February 2024 / Accepted 24 June 2024

Abstract. The effects of absorption and saturation on soliton states in Kerr-type nonlinear layers are theoretically investigated. In addition to the usual gray and bright soliton structures observed in nonlinear slabs, a flat soliton, i.e., a particular soliton excitation with electric field amplitude independent of the position within the layer, is researched in cases of self-defocusing and self-focusing nonlinearities. Effects caused by the combination of absorption and saturation, such as the shift and extinction of the flat soliton peak, the decrease in the amplitude of the electric field within the nonlinear layer, and the suppression of the multistable behavior of the transmission coefficient in the vicinity of the soliton peaks, are discussed. The present theoretical results are compared and found in good quantitative agreement with previous experimental measurements.

Mathematics Subject Classification 35Q60 · 74J35 · 78A60

1 Introduction

The study of solitary waves has aroused great interest in recent decades due to its application in the communications industry. Different approaches for understanding the properties of soliton waves have motivated advances in fields such as mathematics, physics, and biology [1]. According to the concepts of nonlinear optics, solitary electromagnetic waves propagate without energy losses through an optical medium. They originate as a result of different mechanisms such as the photorefractive effect [2]—where electromagnetic waves induce changes in the refractive index—the occurrence of nonlinearities due to thermal effects or molecular orientation [3], and electro-optic effects [4], among others.

From a theoretical point of view, a considerable amount of work has been devoted to studying some features and characteristics of nonlinear systems, such as the bistable behavior of the transmission and reflection coefficients [5], or the transmission properties of electromagnetic waves through nonlinear materials [6]. These researches have also been extended to consider the effects of saturation [6] and absorption [7] on the optical properties of such systems. On the other hand, experimental investigations have been carried out to explore the transmission-switching phenomenon, high transmission states of bistable resonators [8], self-induced transparency in periodic arrays of absorbing dielectrics [9], and so on. Some of the studies have focused on analyzing the transmission properties of electromagnetic waves through nonlinear saturable materials [10], revealing the existence of a hysteresis-like behavior of the transmission coefficient [6].

More recently, we have theoretically investigated soliton excitation in self-defocusing optical layers that exhibit Kerr nonlinearities [11]. We studied the transmission coefficient as a function of the intensity of the incident electromagnetic wave and found that soliton excitations cannot occur when the input intensity exceeds a threshold limit. In that limit, a soliton excitation with spatially independent electric field amplitude can occur within the nonlinear slab, regardless of the value of the incident wave frequency. However, such investigations were carried out without considering the effects of absorption and saturation in the nonlinear medium. The inclusion of such effects in our theoretical framework is now in order. The present work aims to study the effects of absorption and saturation on soliton states in nonlinear layers. We compare our theoretical results with previous experimental measurements [6] on self-focusing nonlinear systems.

The work is organized as follows. In Sect. 2, we present a brief theoretical description of the problem.

C. A. Betancur-Yepes and J. D. Mazo-Vásquez have contributed equally to this work.

[a] e-mail: ndrsbtncr@gmail.com
[b] e-mail: ujjqz@student.kit.edu
[c] e-mail: amador.reyes@udea.edu.co (corresponding author)

Published online: 17 July 2024

Our numerical results are given in Sect. 3, where we compare our main findings with previous experimental measurements by Peschel et al.. Finally, the conclusions are given in Sect. 4.

2 Theoretical framework

We consider a nonlinear slab of thickness d, growth along the z direction, characterized by a magnetic permeability μ and an electric permittivity given by

$$\epsilon = \varepsilon(1 + i\gamma) + \frac{\alpha|\mathcal{E}|^2}{1 + \sigma|\alpha||\mathcal{E}|^2}, \tag{1}$$

where α is the nonlinear dielectric coefficient, ε is the background electric permittivity, γ tunes the absorption properties of the slab, and σ is a positive parameter that accounts for the saturation effect [12] and is related to the upper limit of the refractive index that can be reached optically [10]. The cases $\alpha > 0$ and $\alpha < 0$ correspond to different optical materials that exhibit self-focusing and self-defocusing nonlinearities, respectively.

Suppose that an electromagnetic wave of frequency $\omega = 2\pi\nu$, originating in the linear medium with electric permittivity ε_0 and magnetic permeability μ_0 surrounding the nonlinear layer, is incident on the slab in the transverse-electric configuration [11]. In this way, the electric field component of the wave may be written as $\mathbf{E}(\mathbf{r}, t) = \mathcal{E}(z)e^{i(qx-\omega t)}\mathbf{e}_y$, where $q = \frac{\omega}{c}\sqrt{\mu_0\epsilon_0}\sin(\theta)$ denotes the projection of the wave vector along the x direction, whereas θ is the incidence angle measured in the surrounding medium [11].

According to Maxwell's equations, the electric field amplitude of the electromagnetic wave satisfies the differential equation [13]

$$-\frac{\mathrm{d}}{\mathrm{d}z}\frac{1}{\bar{\mu}(z)}\frac{\mathrm{d}}{\mathrm{d}z}\mathcal{E}(z) = \frac{\omega^2}{c^2}\left[\bar{\varepsilon}(z) - \frac{\mu_0\epsilon_0}{\bar{\mu}(z)}\sin^2(\theta)\right]\mathcal{E}(z), \tag{2}$$

where $\bar{\varepsilon}(z)$ and $\bar{\mu}(z)$ are the position-dependent electric permittivity and magnetic permeability, respectively, such that $\bar{\varepsilon}(z) = \varepsilon_0$ and $\bar{\mu}(z) = \mu_0$ in the surrounding medium, whereas $\bar{\varepsilon}(z) = \epsilon$ [cf. Equ. (1)] and $\bar{\mu}(z) = \mu$ within the nonlinear layer. For simplicity, we have supposed that both $\bar{\varepsilon}$ and $\bar{\mu}$ are independent of the wave frequency. This assumption is a good approximation in experimental situations [6]. We assume:

$$\mathcal{E}(z) = E_i \begin{cases} e^{iQ_0 z} + re^{-iQ_0 z} & \text{if } z < 0 \\ \phi(z) & \text{if } 0 < z < d \\ te^{iQ_0(z-d)} & \text{if } z > d \end{cases}, \tag{3}$$

where E_i is the amplitude of the incident electric field, $Q_0 = \frac{\omega}{c}p_0$, and $p_0 = \sqrt{\varepsilon_0\mu_0}\cos(\theta)$. According to Eqs. (1)–(3), one may obtain the ϕ dimensionless amplitude of the electric field (in units of E_i) within the nonlinear layer from the equation

$$\frac{\mathrm{d}^2}{\mathrm{d}\zeta^2}\phi(\zeta) + \beta^2\phi(\zeta) + \frac{a\mu|\phi(\zeta)|^2\phi(\zeta)}{1 + \sigma|a||\phi(\zeta)|^2} = 0, \tag{4}$$

by taking into account the continuity of both ϕ and $\frac{1}{\mu}\frac{d\phi}{d\zeta}$ at the slab interfaces [11,13]. In the above expression, one has $\zeta = \frac{\omega}{c}z$, $\beta^2 = \varepsilon\mu(1 + i\gamma) - \varepsilon_0\mu_0\sin^2(\theta)$ and $a = \alpha|E_i|^2$ is the so-called normalized input intensity [11]. The reflection (R) and transmission (T) coefficients may be obtained as $R = rr^*$ and $T = tt^*$, respectively. Here, r and t correspond to the electric field amplitudes of the reflected and transmitted waves, respectively, expressed in units of E_i [cf. Equ. (3)].

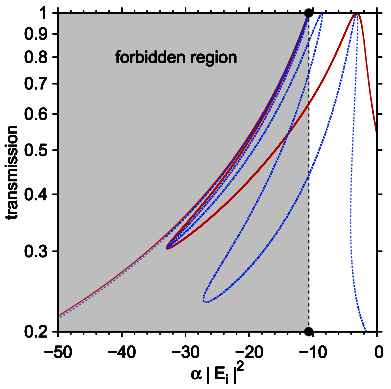

Fig. 1 (Color online) Transmission coefficient as a function of the normalized input intensity $\alpha|E_i|^2$. The obtained results correspond to a self-defocusing material with $d = 5$ mm, $\varepsilon = 11.680$, $\mu = 1.036$, in the absence of both absorption and saturation, and $\theta = \pi/4$. The surrounding optical constants were taken as $\varepsilon_0 = 1$ and $\mu_0 = 1$, so that the conditions $\varepsilon > \mu > \varepsilon_0 = \mu_0$ are fulfilled. Solid and dashed lines correspond to $\nu = 10$ GHz and $\nu = 30$ GHz, respectively. From left to right, the first and second peaks in each case correspond to the flat and gray soliton states, respectively. The vertical dashed line and full dots indicate the value of $a_l < 0$ [cf. Equ. (5)]. The shadow area corresponds to the region of the normalized input intensity where soliton formation is not expected to occur

3 Results and discussion

We begin by analyzing the case of self-defocusing layers previously studied in Ref. [11]. In the absence of absorption and saturation ($\gamma = 0$ and $\sigma = 0$, respectively), the typical Kerr nonlinearity is recovered in Eq. (1) and Eq.(2) can be solved analytically in terms of the elliptic Jacobi functions. In this case, when considering a hypothetical self-defocusing material such that $\varepsilon > \mu > \varepsilon_0 = \mu_0$, we have detailed in a previous work [11] the existence of a normalized input intensity limit below which the formation of soliton states, i.e., electromagnetic waves propagating through the nonlinear layer with $T = 1$, is not possible. Such threshold for the

normalized input intensity, denoted as a_l, is defined by the expression [11]

$$a_l = \frac{\eta^2 - p^2}{\mu}, \tag{5}$$

where $\eta^2 = \frac{\mu^2}{\mu_0^2} p_0^2$ and $p^2 = \varepsilon\mu - \varepsilon_0\mu_0 \sin^2(\theta)$. It should be noted that $a_l < 0$ under the conditions $\varepsilon > \mu > \varepsilon_0 = \mu_0$ [11].

In Fig. 1, we show the transmission spectrum as a function of normalized input intensity, corresponding to a nonlinear self-defocusing layer of thickness $d = 5$ mm, in the absence of absorption and saturation. Calculations were performed by following the analytical method outlined in Ref. [11], for $\varepsilon = 11.680$, $\mu = 1.036$, $\varepsilon_0 = 1$, $\mu_0 = 1$, $\theta = \frac{\pi}{4}$, and for two different values of wave frequency. The vertical dashed line and solid dots indicate the value of a_l. The shadow area corresponds to the region of the normalized input intensity where soliton formation is not expected to occur. According to Ref. [11], the transmission coefficient in the absence of absorption and saturation tends toward one in the limit $\alpha|E_i|^2 \to a_l$ (cf. Fig. 1). Therefore, a_l is not only the threshold of the normalized input intensity determining the formation of solitons within the nonlinear layer but also the position of a particular soliton peak in the transmission spectrum as a function of the normalized input intensity. Regardless of the wave frequency value, such a peak of T comes from an electromagnetic state with a spatially independent electric field amplitude [11]. In contrast with the bright, dark, or gray stationary solitons [14] that may exist within the nonlinear slab, we have termed this state the flat soliton state. In this way, Eq. (5), which is the condition for the occurrence of this flat soliton, may be rewritten as

$$\frac{a_l}{\mu} = \frac{1}{Z_0^2} - \frac{1}{Z^2} + \left(\frac{\mu_0^2}{\mu^2} - 1\right) \frac{1}{Z_0^2} \sin^2(\theta), \tag{6}$$

where $Z_0 = \sqrt{\frac{\mu_0}{\varepsilon_0}}$ is the optical impedance of the surrounding medium, whereas $Z = \sqrt{\frac{\mu}{\varepsilon}}$ is the background optical impedances of the nonlinear layer. From the above expression, it follows that, in the case of normal incidence, the a_l normalized input intensity to obtain the flat soliton must be proportional to the difference between the inverse square of the optical impedances of the surrounding medium and the background. For oblique incidence, a_l depends on the incidence angle, except if $\mu = \mu_0$. In any case, this soliton state is solely determined by the optical properties of the surrounding medium and the nonlinear layer. Still, it is independent of the slab width and also of the wave frequency in the case of non-dispersive materials.

To better understand the nature of the flat soliton, we emphasize that Eq. (6) provides a condition to obtain fully transmitted optical states through the nonlinear layer. To analyze Eq. (6), we first consider the linear regime ($\alpha = 0$) and normal incidence ($\theta = 0$). In this case, we have $a_l = 0$ and, therefore, Eq. (6) leads to

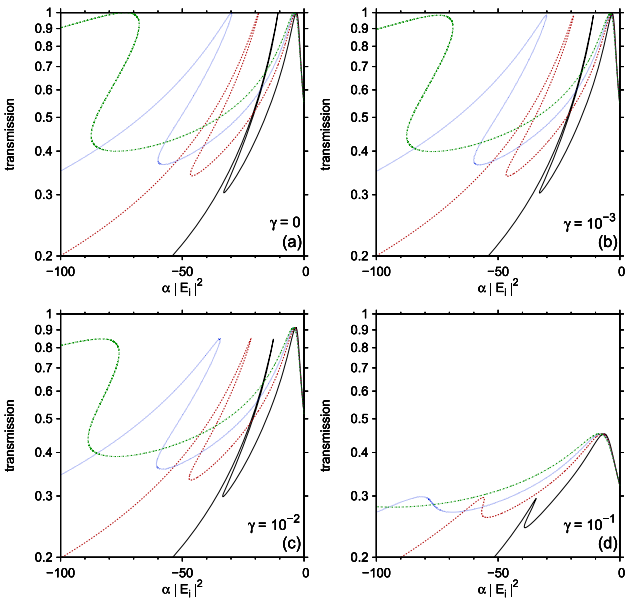

Fig. 2 (Color online) Transmission coefficient as a function of the normalized input intensity $\alpha|E_i|^2$ for $\nu = 10$ GHz and different values of the γ absorption parameter. The results correspond to a self-defocusing material with $d = 5$ mm, $\varepsilon = 11.680$, $\mu = 1.036$, and $\theta = \pi/4$. The surrounding optical constants were taken as $\varepsilon_0 = 1$ and $\mu_0 = 1$. Solid, dashed, dotted, and dotted–dashed lines correspond to $\sigma = 0$, $\sigma = 0.04$, $\sigma = 0.06$, and $\sigma = 0.08$, respectively. From left to right, the first and second peaks in each case correspond to the flat and gray soliton states, respectively

$Z_0^2 = Z^2$. It has been established that, for normal incidence, the impedance matching of two different linear optical media leads to the suppression of the reflected wave at the interface between them [15] and the increase in the transmissivity. A similar effect was observed in disordered linear photonic heterostructures under normal incidence, where the impedance matching of the optical media across the growth direction leads to the suppression of the Anderson localization of light in such systems [16]. In the case of oblique incidence, Eq. (6) can be rewritten as

$$\sin^2(\theta) = \frac{\frac{a_l}{\varepsilon_0} + \frac{\varepsilon}{\varepsilon_0} - \frac{\mu}{\mu_0}}{\frac{\mu}{\mu_0} - \frac{\mu_0}{\mu}}. \tag{7}$$

In the linear regime ($a_l \to 0$), Eq. (7) becomes the standard formula describing the Brewster effect for waves incident with transverse-electric polarization [17]. In such a case, the reflected wave also vanishes, and the transmissivity reaches the maximum value.

The above evidence allows us to conclude that, in the nonlinear regime, the presence of the flat soliton occurring in a_l is a consequence of the properties of the linear/nonlinear interface and not of the geometric properties of the optical system. Furthermore, the independence of a_l on the wave frequency is a consequence of the fact that the optical impedances of the incident medium and the background impedance of the nonlin-

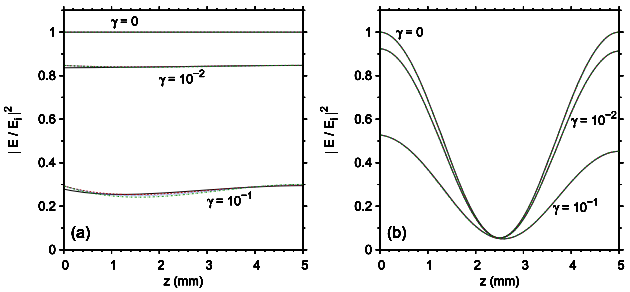

Fig. 3 (Color online) Square of the electric field amplitude, as a function of the position within the nonlinear layer, for different values of the γ absorption parameter. The results in panels (**a**) and (**b**) are related to the first (flat) and second (gray) soliton peaks, respectively, observed in the transmission spectrum shown in Fig. 2 for the corresponding values of γ and σ. The calculations were performed for $\nu = 10$ GHz, $\theta = \pi/4$, and $\varepsilon_0 = \mu_0 = 1$, in a self-defocusing optical layer of width $d = 5$ mm, $\varepsilon = 11.680$, and $\mu = 1.036$. Solid, dashed, dotted, and dotted–dashed lines correspond to $\sigma = 0$, $\sigma = 0.04$, $\sigma = 0.06$, and $\sigma = 0.08$, respectively

ear medium are independent of the wave frequency. In contrast with the flat soliton, the other soliton states obtained from the transmission peaks on the right side of a_l (cf. Fig. 1) depend on the geometry of the slab, i.e., of the slab thickness, as detailed in Ref. [11].

To complete the study of the soliton properties by simulating more real experimental conditions, we have investigated the nonlinear modes, particularly the flat soliton in systems where the absorption and saturation parameters differ from zero. In the presence of absorption and saturation, Eq. (4) cannot be solved analytically. Hence, it is necessary to implement numerical procedures to calculate the transmission coefficient of the system. We have followed the recipe outlined in Ref. [13] and used a fourth-order Runge–Kutta method to solve Eq. (4) and calculate the transmission coefficient as a function of the normalized input intensity. All the theoretical results from Figs. 2, 3, 4, 5, 6, 7 were numerically obtained within such a scheme.

The transmission coefficient corresponding to a self-defocusing slab of thickness $d = 5$ mm, as a function of the normalized input intensity $\alpha|E_i|^2$, is shown in Fig. 2 for different values of the absorption parameter γ. Results were numerically obtained for $\nu = 10$ GHz, oblique incidence with $\theta = \pi/4$, and for the same values of ε, μ, ε_0, μ_0 that we used in Fig. 1. Solid, dashed, dotted, and dotted–dashed lines correspond to $\sigma = 0$, $\sigma = 0.04$, $\sigma = 0.06$, and $\sigma = 0.08$, respectively. The square of the electric field amplitudes, for the respective values of σ and γ, is shown in Fig. 3. Figure 3a and b corresponds to the first and second peaks, counting from left to right, shown in Fig. 2. Results are given in units of the electric field amplitude of the incident wave and displayed as functions of the position within the slab.

In the absence of absorption, it is apparent from Fig. 3 that the first and second peaks in the transmission spectrum correspond to flat and gray soliton states, respectively. In this case ($\gamma = 0$), the soliton is an electromagnetic state transmitted through the nonlinear slab with $T = 1$. Therefore, due to the symmetry of Eq. (2), the square of the amplitude of the electric field must also exhibit an inversion symmetry with respect to the center of the slab [18]. The presence of absorption within the nonlinear layer leads to the suppression of the condition $T = 1$, to a drop in the transmission coefficient, and, therefore, to a destruction of the soliton state. However, the structure of the electric field amplitude observed in Fig. 3 for $\gamma > 0$ still approximately preserves inversion symmetry, mainly for the lower values of γ ($\sim 10^{-2}$ or less). Although the height of the transmission peaks decreases as γ increases (cf. Fig. 2), the absorption effects are more noticeable in the flat soliton peak than in the gray soliton peak. Such a fact could hinder the experimental observation of the flat soliton.

For all absorption levels considered here, the positions of the soliton peaks in the transmission spectrum shift to lower values of a as the saturation parameter increases. In all cases, the transmission peaks depend on σ, but such dependence is most remarkable for the flat soliton peak. The shift of the first peak can be described by an inverse power function of σ, whereas the position of the second peak behaves approximately as a linear function of the saturation parameter (results not shown here). Even though the transmission peaks depend on the saturation parameter, the square of the electric field amplitudes displayed in Fig. 3 is almost independent of σ. Although Eq. (5) (or Eq. (6), equivalently) is not valid in the presence of absorption or saturation, no soliton states are observed to the left of the first (flat soliton) peak of the transmission spectrum depicted in each panel of Fig. 2.

One of the most dramatic effects of saturation in the transmission spectrum is the loss of the multistability that the transmission coefficient presents for specific values of σ, that is, the suppression of the possibility of obtaining different transmission values for a single value of the normalized input intensity. Figure 2d, for example, shows that for $\sigma > 0.06$, the multistability around the flat soliton peak is lost. Thus, the correct combination of the parameters γ and σ can destroy the multistable behavior of the transmission spectrum. The experimental observation of multistability would depend on the specific values of the optical parameters of the actual material used to build the slab.

We now turn to the case of self-focusing nonlinear layers by considering a hypothetical material such that $\varepsilon_0 > \mu_0 > \varepsilon = \mu$. Under such conditions, it can be seen from Eq. (6) that $a_l > 0$. For computational purposes, we have chosen $\varepsilon = \mu = 1$ for the background optical constants of the nonlinear slab, whereas $\varepsilon_0 = 11.680$ and $\mu_0 = 1.036$ in the surrounding medium. The transmission coefficient, as a function of the normalized input intensity, is shown in Fig. 4 for two different values of the wave frequency. Results were numerically obtained for a self-focusing layer of thickness $d = 5$ mm and for $\theta = \pi/4$ in the absence of both absorption and saturation. The vertical dashed line and solid

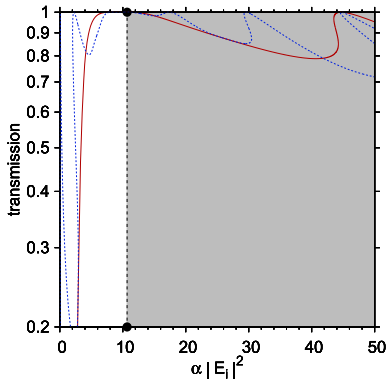

Fig. 4 (Color online) Transmission coefficient as a function of the normalized input intensity $\alpha|E_i|^2$. The results correspond to a self-focusing slab with $d = 5$ mm, $\varepsilon = \mu = 1$, $\sigma = \gamma = 0$, and $\theta = \pi/4$. The surrounding optical constants were taken as $\varepsilon_0 = 11.680$, $\mu_0 = 1.036$ in such a way that $\varepsilon_0 > \mu_0 > \varepsilon = \mu$. Solid and dashed lines correspond to $\nu = 10$ GHz and $\nu = 30$ GHz, respectively. The vertical dashed line and full dots indicate the value of $a_l > 0$ [cf. Equ. (5)]. The white (shadow) area corresponds to the region of the normalized input intensity where bright (gray) solitons can occur

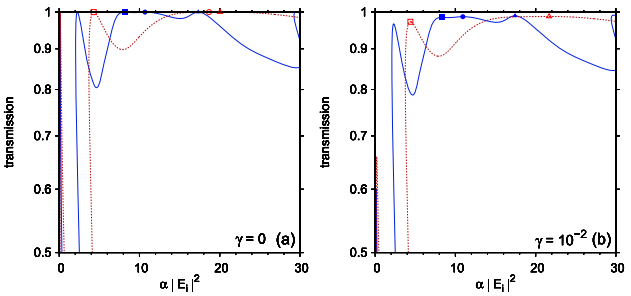

Fig. 5 (Color online) Transmission coefficient as a function of the normalized input intensity $\alpha|E_i|^2$ for $\nu = 30$ GHz and two different values of the γ absorption parameter. The results correspond to a self-focusing material with $d = 5$ mm, $\varepsilon = \mu = 1$, and $\theta = \pi/4$. The surrounding optical constants were taken as $\varepsilon_0 = 11.680$ and $\mu_0 = 1.036$ to fulfill the conditions $\varepsilon_0 > \mu_0 > \varepsilon = \mu$. Solid lines and solid symbols correspond to $\sigma = 0$, whereas dashed lines and open symbols correspond to $\sigma = 0.04$. Squares and triangles are used to identify the bright and gray soliton peaks, respectively, whereas circles correspond to flat soliton peaks in the transmission spectrum. The flat soliton peak in panel (b) is not observed for $\sigma = 0.04$

dots indicate the value of $a_l > 0$. In contrast with the previous case, where in the absence of both absorption and saturation, the values of a_l correspond to the normalized input intensity threshold for the existence of solitons and also to the flat soliton peak position, it is apparent from Fig. 4 that soliton excitations can occur even if $0 < \alpha|E_i|^2 < a_l$. Transmission peaks in this region correspond to bright soliton states, whereas only gray solitons can exit in the region $\alpha|E_i|^2 > a_l$ (see below). The transmission coefficient still exhibits a maximum at $\alpha|E_i|^2 = a_l$, which corresponds to the

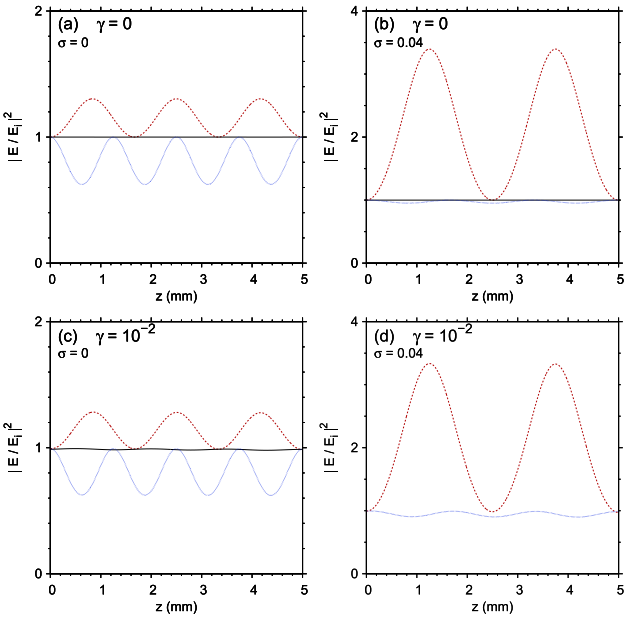

Fig. 6 (Color online) Square of the electric field amplitude, as a function of the position within the nonlinear layer, for different values of both the absorption parameter γ and the saturation parameter σ. The calculations were performed for $\nu = 30$ GHz, $\theta = \pi/4$, $\varepsilon_0 = 11.680$, and $\mu_0 = 1.036$, in a self-focusing optical layer of width $d = 5$ mm and $\varepsilon = \mu = 1$. The dashed, solid, and dotted lines in panel (**a**) [(**b**)] correspond to the bright, flat, and gray solitons, respectively, obtained for the values of $\alpha|E_i|^2$ corresponding to the solid (open) square, circle, and triangle, respectively, shown in Fig. 5a, for $\sigma = 0$ ($\sigma = 0.04$) and $\gamma = 0$. The same applies to panel (**c**) [(**d**)], corresponding to the square of the electric field amplitude obtained from the solid (open) symbols depicted in Fig. 5b, for $\sigma = 0$ ($\sigma = 0.04$) and $\gamma = 10^{-2}$. The flat soliton in panel (d) is absent [cf. the absence of the flat soliton peak in Fig. 5b]

flat soliton state. In this sense, the white and shaded regions shown in Fig. 4 correspond to the normalized input intensity regions where bright and gray solitons can occur, respectively.

The previously described behavior of soliton states is also observed in the presence of low levels of both absorption and saturation. To further clarify this, we show in Fig. 5 the transmission coefficient, as a function of the normalized input intensity, corresponding to a self-focusing material with $d = 5$ mm. The calculation parameters were taken as $\nu = 30$ GHz, $\theta = \pi/4$, $\varepsilon = \mu = 1$, $\varepsilon_0 = 11.680$ and $\mu_0 = 1.036$. The results shown in Fig. 5a and b correspond to $\gamma = 0$ and $\gamma = 10^{-2}$, respectively. Solid and dashed lines in all panels correspond to $\sigma = 0$ and $\sigma = 0.04$, respectively. The amplitude of the electric field can be obtained by evaluating the numerical solution of Eq. (2) at the position of the transmission peaks, leading to the soliton states. In this way, we show in Fig. 6 the square of the electric field amplitude as a function of the position within the nonlinear layer, corresponding to the soliton peaks identified by symbols in Fig. 5. The solid lines

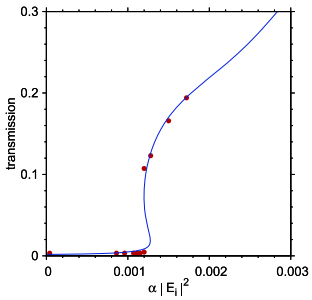

Fig. 7 (Color online) Transmission coefficient, as a function of the normalized input intensity $a|E_i|^2$, in self-focusing optical layers experimentally studied by Peschel et al. [6]. Solid lines correspond to present theoretical results, whereas full circles correspond to experimental measurements [6] of the transmission coefficient (see text)

shown in Fig. 6a and b represent the square of the electric field amplitudes at the values of $\alpha|E_i|^2$ corresponding to the solid and open circles, respectively, which are shown in Fig. 5a. These electromagnetic states are flat solitons for $\sigma = 0$ and $\sigma = 0.04$, respectively, in the absence of absorption. The position of the full circle on the horizontal axis in Fig. 5a corresponds exactly to the value of a_l [see Eq. (5)]. The dashed and dotted lines in Fig. 6a [b] represent the bright and gray solitons, respectively, obtained by evaluating the solution of Eq. (2) at the transmission peaks identified by the solid (open) square and triangle, respectively, shown in Fig. 5a for $\sigma = 0$ ($\sigma = 0.04$) and $\gamma = 0$. For the absorption level corresponding to $\gamma = 10^{-2}$, bright and gray solitons (dashed and dotted lines, respectively) are also observed in Fig. 6c [d] in the case of $\sigma = 0$ ($\sigma = 0.04$). Similarly, the results were obtained from the transmission peaks corresponding to the solid (open) square and triangle, respectively, in Fig. 5b. Figure 5b shows that the flat soliton peak in the transmission spectrum can only be observed for $\sigma = 0$. The flat soliton peak fades out dramatically for relatively low absorption levels as σ increases (results not shown here), and it is absent from the transmission spectrum obtained for $\sigma = 0.04$ [cf. dashed line in Fig. 5b]. Therefore, there is no flat soliton to observe in Fig. 6d. Once again, the combined effects of absorption and saturation can cause a drastic change in the transmission spectrum, including the complete extinction of the flat soliton peak if σ and γ increase enough.

It is desirable to validate our theoretical model by comparing the present numerical results and the experimental measurements of the transmission coefficient in Kerr-type nonlinear layers. Although we have not found suitable experiments on self-defocusing systems similar to the one considered here, the transmission properties of nonlinear self-focusing layers were experimentally investigated in a pioneering work by Peschel et al. [6]. Then we compared in Fig. 7 our theoretical results for $a > 0$ (solid line) and the experimental data (full dots) by Peschel et al.. The experimental setup consisted of a liquid crystal thin film [p-methoxybenzylidene-p-n-butylaniline (MBBA)] sandwiched between two linear dielectrics. The experimental parameters were $d = (6 \pm 1)$ μm, $\varepsilon = 2.460 \pm 2 \times 10^{-3}$, $\epsilon_0 = 2.4650 \pm 2 \times 10^{-4}$, $\mu = \mu_0 = 1$, $\theta = 88.0° \pm 0.1°$, and $\nu = 614.75$ THz. According to Ref. [6], the nonlinear dielectric coefficient can be estimated by the expression $\alpha = \varepsilon_0 \varepsilon c n_{2I}$, where $n_{2I} = 10^{-9}$ m^2/W [19] accounts for the nonlinear Kerr contribution to the refractive index. The numerical calculation was performed with the same parameters except for the layer thickness and the incidence angle. To better fit the experimental results, we chose $d = 7$ μm and $\theta = 87.9°$, values within the corresponding estimated ranges of these magnitudes. Note that the experimental errors of d and θ are 1 μm and 0.1°, respectively [6]. In addition, we set $\gamma = 3.8 \times 10^{-4}$ and $\sigma = 10$. The good agreement between the experimental and theoretical results is shown in Fig. 7. In this sense, the available experimental results validate our theoretical model to investigate the transmission and soliton properties of nonlinear optical layers.

4 Conclusions

In summary, we have theoretically investigated the effects of absorption and saturation on soliton states in Kerr-type nonlinear layers. In self-defocusing Kerr materials with relatively low levels of absorption and saturation, we have shown that soliton excitations cannot occur if the normalized input intensity is below a well-defined cutoff value. In this limit, the transmission coefficient, computed as a function of the normalized input intensity, shows a sharp peak corresponding to a flat soliton. This particular electromagnetic state is neither a bright nor a dark soliton in the traditional sense [14], and its electric field amplitude is almost independent of the spatial position within the nonlinear layer regardless of the wave frequency value. We also observed a strong dependence of the flat soliton peak position, in the transmission spectrum as a function of the normalized input intensity, on the saturation parameter. In contrast, the amplitude of the electric field is almost independent of the saturation for low absorption levels. Moreover, an increase in the absorption parameter can cause the flat soliton peak in the transmission spectrum to fade away. It may also lead to a considerable decrease in the electric field amplitude corresponding to the flat soliton.

In the case of self-focusing Kerr nonlinearity, there is no limit on the normalized input intensity for the excitation of solitons within the layer. The flat soliton peak is still observed in the transmission spectrum as a function of the normalized input intensity. We obtained only bright solitons for normalized input intensities less than the position of the flat soliton peak. In contrast, gray solitons were observed for normalized input intensities greater than such peak position in the transmission spectrum. We emphasize that, in both the self-defocusing and self-focusing layers, absorption and saturation effects can cause drastic changes in the trans-

mission spectrum and eventually lead to the complete extinction of the flat soliton when σ y γ is large enough. Furthermore, a simultaneous increase in the absorption and saturation levels can destroy the multistable behavior of the transmission coefficient as a function of the normalized input intensity. Finally, the theoretical results corresponding to the self-focusing case were compared with previous experimental measurements by Peschel et al. [6]. The excellent agreement between experiment and theory validates the present model and its predictions. We hope this study will stimulate future experiments on this topic.

Author contributions

All the authors have performed the calculations, written the paper, and revised it before submission.

Funding Open Access funding provided by Colombia Consortium. This work was partially supported by the Scientific Colombian Agency CODI—University of Antioquia. J. D. Mazo-Vásquez is part of the Max Planck School of Photonics, supported by the German Federal Ministry of Education and Research (BMBF), the Max Planck Society, and the Fraunhofer Society.

Data Availability Statement This manuscript has no associated data, or the data will not be deposited. [Authors' comment: The data sets generated during and/or analyzed during the current study are available from the corresponding author on reasonable request.]

References

1. A.S. Davydov, Solitons, in *Modern Problems in Condensed Matter Sciences*, vol. 17, ed. by S.E. Trullinger, V.E. Zakharov, V.L. Pokrovsky (Elsevier, Amsterdam, 1986), pp.1–51
2. P. Yeh, *Introduction to Photorefractive Nonlinear Optics. Wiley Series in Pure and Applied Optics* (Wiley, Hoboken, 1993)
3. C.H. Kwak, G.Y. Kim, Rigorous theory of molecular orientational nonlinear optics. AIP Adv. **5**(1), 017124 (2015). https://doi.org/10.1063/1.4906521
4. Z. Jiang, C. Paillard, H. Xiang, L. Bellaiche, Linear versus nonlinear electro-optic effects in materials. Phys. Rev. Lett. **125**, 017401 (2020). https://doi.org/10.1103/PhysRevLett.125.017401
5. K.M. Leung, Exact results for the scattering of electromagnetic waves with a nonlinear film. Phys. Rev. B **39**, 3590–3598 (1989). https://doi.org/10.1103/PhysRevB.39.3590
6. T. Peschel, P. Dannberg, U. Langbein, F. Lederer, Investigation of optical tunneling through nonlinear films. J. Opt. Soc. Am. B **5**(1), 29–36 (1988). https://doi.org/10.1364/JOSAB.5.000029
7. E. Reyes-Gómez, S.B. Cavalcanti, L.E. Oliveira, Absorption effects on plasmon polariton-gap solitons in kerr/metamaterial superlattices. Europhys. Lett. **106**(6), 64001 (2014). https://doi.org/10.1209/0295-5075/106/64001
8. Z. Chai, X. Hu, F. Wang, X. Niu, J. Xie, Q. Gong, Ultrafast all-optical switching. Adv. Opt. Mater. **5**(7), 1600665 (2017). https://doi.org/10.1002/adom.201600665
9. A. Kozhekin, G. Kurizki, Self-induced transparency in bragg reflectors: gap solitons near absorption resonances. Phys. Rev. Lett. **74**, 5020–5023 (1995). https://doi.org/10.1103/PhysRevLett.74.5020
10. S. Gatz, J. Herrmann, Soliton propagation in materials with saturable nonlinearity. J. Opt. Soc. Am. B **8**(11), 2296–2302 (1991). https://doi.org/10.1364/JOSAB.8.002296
11. L.M. Hincapie-Zuluaga, J.D. Mazo-Vásquez, C.A. Betancur-Silvera, E. Reyes-Gómez, Transmission of electromagnetic waves through nonlinear optical layers. EPL (Europhysics Letters) **134**(5), 54002 (2021). https://doi.org/10.1209/0295-5075/ac0ad7
12. S. Hu, W. Hu, Defect solitons in saturable nonlinearity media with parity-time symmetric optical lattices. Physica B **429**, 28–32 (2013). https://doi.org/10.1016/j.physb.2013.07.023
13. S.B. Cavalcanti, P.A. Brandão, A. Bruno-Alfonso, L.E. Oliveira, Bulk plasmon polariton-gap soliton-induced transparency in one-dimensional kerr-metamaterial superlattices. Opt. Lett. **39**(1), 178–181 (2014). https://doi.org/10.1364/OL.39.000178
14. Y.S. Kivshar, B. Luther-Davies, Dark optical solitons: physics and applications. Phys. Rep. **298**(2), 81–197 (1998). https://doi.org/10.1016/S0370-1573(97)00073-2
15. M. Mazilu, K. Dholakia, Optical impedance of metallic nano-structures. Opt. Express **14**(17), 7709–7722 (2006). https://doi.org/10.1364/OE.14.007709
16. E. Reyes-Gómez, A. Bruno-Alfonso, S.B. Cavalcanti, L.E. Oliveira, Suppression of anderson localization of light in one-dimensional disordered photonic superlattices. Phys. Rev. B **85**, 195110 (2012). https://doi.org/10.1103/PhysRevB.85.195110
17. C. Fu, Z.M. Zhang, P.N. First, Brewster angle with a negative-index material. Appl. Opt. **44**(18), 3716–3724 (2005). https://doi.org/10.1364/AO.44.003716

18. E. Reyes-Gómez, S.B. Cavalcanti, L.E. Oliveira, Non-bragg-gap solitons in one-dimensional kerr-metamaterial fibonacci heterostructures. Phys. Rev. E **91**, 063205 (2015). https://doi.org/10.1103/PhysRevE.91.063205

19. H. Vach, C.T. Seaton, G.I. Stegeman, I.C. Khoo, Observation of intensity-dependent guided waves. Opt. Lett. **9**(6), 238–240 (1984). https://doi.org/10.1364/OL.9.000238